



HAL
open science

Effect of grain direction on cutting forces and chip geometry during green beech wood machining

Rémi Curti, Bertrand Marcon, Louis Denaud, Robert Collet

► **To cite this version:**

Rémi Curti, Bertrand Marcon, Louis Denaud, Robert Collet. Effect of grain direction on cutting forces and chip geometry during green beech wood machining. *Bioresources*, 2018, 13 (3), pp.5491-5503. hal-01809144

HAL Id: hal-01809144

<https://hal.science/hal-01809144>

Submitted on 6 Jun 2018

HAL is a multi-disciplinary open access archive for the deposit and dissemination of scientific research documents, whether they are published or not. The documents may come from teaching and research institutions in France or abroad, or from public or private research centers.

L'archive ouverte pluridisciplinaire **HAL**, est destinée au dépôt et à la diffusion de documents scientifiques de niveau recherche, publiés ou non, émanant des établissements d'enseignement et de recherche français ou étrangers, des laboratoires publics ou privés.

Effect of Grain Direction on Cutting Forces and Chip Geometry during Green Beech Wood Machining

Rémi Curti,* Bertrand Marcon, Louis Denaud, and Robert Collet

Proper valorization of the sawing wastes in industrial sawmills is a permanent issue with strong economic and environmental stakes. Most industrial sawmills are equipped with chipper-canter heads reducing the outer part of the logs into chips used in the pulp and paper industry. Optimization in canter use would increase the acceptable proportion of exploitable chips for this industry. With chipper-canters, the cutting direction varies along the cut. This study investigates the impact of the angle formed between the cutting direction and the grain direction on the required cutting force and the chips' geometry. Orthogonal cutting is conducted to simulate the chipper-canter machining operation on green beech. To lower the cutting forces when machining, aiming for a cutting direction as parallel as possible to the wood fiber is necessary. However, if this angle is too low, the chips' generated geometries prevent them from a proper valorization of this resource. A compromise with grain direction between 50° to 70° both limits the cutting forces and improves the steadiness of the chip fragmentation.

Keywords: Green wood; Orthogonal cutting; Cutting forces; Chip fragmentation; Ultra-fast imaging; Wood chips

Contact information: LaBoMaP (EA 3633), Arts et Métiers, Rue Porte de Paris, 71250 Cluny, France;
* *Corresponding author:* remi.curti@ensam.eu

INTRODUCTION

Among the products of French sawmills—barks, slabs, edgings, sawdust, and chips—chips have the most consistent added value. In 2015, 2,370 kilotons (16%) of the 14,800 kilotons (dry, debarked) of wood gathered and commercialized in France ended up in chips and slabs sold by sawmills to papermakers (COPACEL 2016; FCBA 2017). Despite this large figure, sawmills have difficulty selling their chips to paper producers. The chips are often rejected due to their geometry and especially their non-compliant thickness. As a consequence, they are burnt to produce energy, which is a poor economic exploitation. To promote their waste valorization, industrial sawmills must obtain new tools to predict chip characteristics, such as their geometry. Chip thickness, which is the most difficult dimension to calibrate, is also a highly regarded quality criterion in the paper industry supply (Akhtaruzzaman and Virkola 1979; Brännvall 2017). In sawmills, most chips are produced by chipper-canters. Chipper-canters are large conical mills on which several knives are clamped. They transform logs into cants, shredding the slabs (cylindrical parts of the logs) into chips. The geometry of the chips generated and the cutting forces induced by the process vary according to multiple parameters.

The first parameters to impact the two aforementioned physical quantities are material-related: the wood species (Hernandez and Quirion 1995), its density (Eyma 2002), its moisture content, and its temperature. However, Hernández *et al.* (2014) showed that above 0 °C, the moisture content of the wood does not significantly impact the mechanical properties inducing the chip fragmentation mechanisms. The type of wood (reaction,

tension, compression, early, or late) might also have an influence, but this has not been determined.

The second parameter set to modify the geometry of the chips and the cutting forces is process-based. These parameters are feed per tooth (Twaddle 1997; Felber and Lackner 2005; Curti *et al.* 2017), which can be assimilated to chip length when the cutting direction is perpendicular to the fiber, cutting speed (Hernandez and Boulanger 1997; Laganière 2004), cutting direction (Kuljich *et al.* 2013), and feed rate (Laganière 2004).

The last main impacting parameters are related to the tool. The tool rake angle was studied by Kuljich *et al.* (2013), and the wear of the tool was studied by Ghosh *et al.* (2015). Nati *et al.* (2010) also showed that in the case of industrial chippers the tool wear increases the proportion of large chips. Material and/or type of coating of the knife or its clearance angle have not been investigated yet, even though these parameters have been widely studied for other purposes like tool life duration. Others parameters exist, but their significance appears to be very low or situational.

Among the aforementioned parameters, the angle between the cutting direction and the grain direction (*GD*) impacts the chip thickness and varies a lot during the cut. This angle changes the cutting mechanism involved in the chip splitting (McKenzie 1960). Focusing on the balsam fir wooden species, Kuljich *et al.* (2013) highlighted the impact of a 45° variation in the cutting direction on the cutting forces and the surface integrity of the specimen after machining. For this reason, on some chipper-canter lines, the in-feed log conveyor height can be set up to modify the knives' working angle; this makes it possible to act on the cutting direction (Laganière 2004; Kuljich *et al.* 2017) by providing an additional way to control the process.

The present work draws attention to this angle's impact on both the cutting forces and the generated chips' thickness when machining beech green wood. Beech green wood is a widely sawn species in Western European sawmills. Moreover, it is very homogeneous (toward softwoods) with small growth rings. Those two properties permit investigation of these factors with smaller scaled samples. The cutting experiments were conducted in planing, as a simplified process. In order to highlight cutting mechanisms and properly design the experiments, orthogonal cutting was chosen over canting. This operation also allowed the studied parameters to be isolated; the fiber angle was changed without affecting the other cutting parameters such as the cut section, which is continuously changed during canting. In orthogonal cutting, the cutting direction is invariant, so *GD* is the variable parameter used to act on the angle formed by those two directions according to the following rule: when the cutting direction is parallel to the fiber, $GD = 0^\circ$.

EXPERIMENTAL

Materials

Experiments were conducted on green beech specimens. One beech log was flat sawn into 1 m long planks. Every plank was then machined into 10 mm-thick boards. Centered in each board, up to nine $100 \times 105 \times 10 \text{ mm}^3$ specimens were machined with various orientations on a Computer Numerical Control routing machine Record 1 (SCM, Rimini, Italy), resulting in a total of 56 specimens. The moisture content (*MC*) and specific gravity (*SG*) of each specimen were computed from Eq. 1 and Eq. 2, respectively,

$$MC = \frac{m_{\text{green}} - m_{\text{ovendry}}}{m_{\text{ovendry}}} \times 100, \quad (1)$$

$$SG = \frac{m_{\text{ovendry}}}{V_{\text{saturated}} \times \rho_{\text{water}}}, \quad (2)$$

where m_{green} is the mass of the specimen measured right after the cutting experiment (approximately 1 min), m_{ovendry} is the mass of the specimen measured after drying in an oven until the difference between two 4-h consecutive measurements is less than 0.5%, $V_{\text{saturated}}$ is the volume of the specimen saturated by water, and ρ_{water} is the density of water. This last quantity was measured by using Archimedes' principle, following the recommendations of Williamson and Wiemann (2010). The mean MC of the specimens was 69.44%, with a standard deviation of 13.39%, and SG was equal to 0.52 ± 0.03 .

Orthogonal Cutting Set-Up and Instrumentation

Orthogonal cutting experiments were conducted with a 3-axes CNC milling center DMC 85 VL (DMG MORI Aktiengesellschaft, Bielefeld, Germany) in which axes were powered by linear motors, allowing for a maximum cutting speed of 2 m s^{-1} . Since usual chipper-canter cutting speeds are between 40 m s^{-1} and 60 m s^{-1} , this available speed was fairly low. However, 15 complimentary cutting experiments over one decade of cutting speed (between 0.2 m s^{-1} and 2 m s^{-1}) were run without significant impact on the measured forces. The specimens were clamped in the spindle head with a self-designed stiff fixture composed of an angle bracket and a vise. The cut was operated by a static single chipper-canter tooth screwed onto a 3-component piezoelectric dynamometer 9255A (KISTLER GROUP, Winterthur, Switzerland) that was clamped itself on the CNC table. The cutting speed (V_c) for all experiments was 2 m s^{-1} , and the chosen uncut chip thickness was $h = 10 \text{ mm}$. Considering the specimen thickness (b) of 10 mm , which was also equal to the cutting width of the operation, the cut section was $10 \times 10 \text{ mm}^2$. Using an analogy with milling, the uncut chip thickness corresponds to the feed per tooth, and the cutting width corresponds to the depth of cut. The chips produced by canters present on average a higher section (around $30 \times 40 \text{ mm}^2$, although it can vary greatly from one operation to another), but the motors of the machine did not permit a higher section to be cut without risk of stalling.

The whole cutting process was recorded by an ultra-fast camera FastCAM SA-Z (PHOTRON, Tokyo, Japan) mounted with a telecentric lens and extension tubes to set the desired observation field of $18 \times 18 \text{ mm}^2$. Due to the speed of the experiments, the shutter time was low ($1/40,000 \text{ s}$ in the present case) to access very clear frames with no blur. Due to the short exposition time, the observed area was strongly enlightened by 10 high power LEDs (3200 lumens each), where the light was directed and focused through optical fibers (Fig. 1).

This setup allowed for each cutting experiment the following to be recorded: 6 force signals (resultants and momentum in all 3 directions of space) and 1,400 images (one image each $5 \times 10^{-5} \text{ s}$, also equivalent to one image every 0.1 mm of specimen displacement). In addition, the position of the machine head in the cutting direction was directly recorded with an incremental coder and used to trigger the imager when the specimen passed through the camera's field of observation. All signals were synchronized thanks to acquisition cards mounted on a chassis cDAQ9188 (National Instruments, Austin, USA). The experimental conditions are summarized in Table 1.

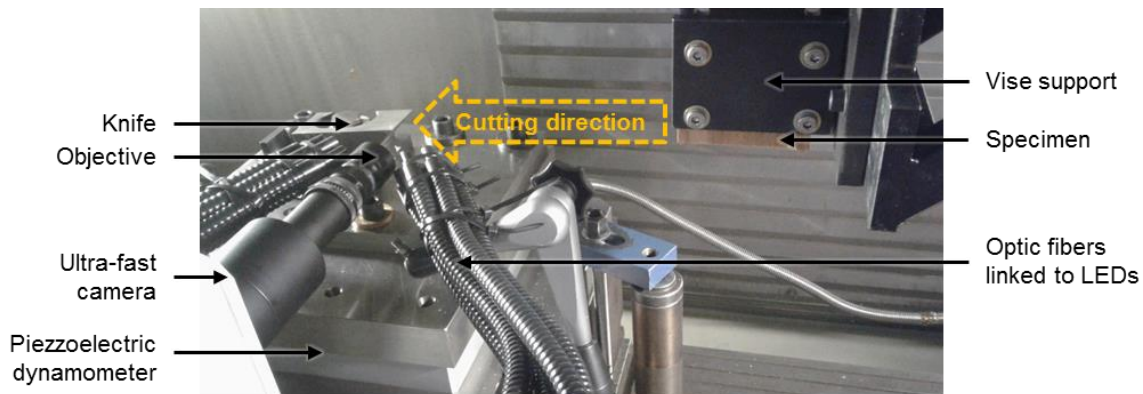


Fig. 1. Experimental setup and instrumentation

Table 1. Experimental Parameters

Trial Parameters	Values	Sensors Parameters	Values
Cutting speed (V_c)	2 m s^{-1}	Sampling rate	20,000 Hz
Uncut chip thickness (h)	10 mm	Frame per second	20,000 fps
Cutting width (b)	10 mm	Shutter time	$1/40,000 \text{ s}$
Rake angle	45°	Definition	$1,024 \times 1,024 \text{ pixels}^2$
Clearance angle	5°	Resolution	$17.58 \times 17.58 \mu\text{m}^2$

Experimental Plan: Study Area and Grain Directions

To quantify the impact of cutting angle on the chip thickness and the cutting forces, specimens presenting 11 different targeted grain directions (GD_{th}) from 10° to 110° by 10° steps (6 repetitions) were machined. The first eight of them, from 40° to 110° , were tested with six repetitions. The three other targeted grain directions (10° , 20° , and 30°) were tested with fewer repetitions (respectively 2, 3, and 3) because they are unusually encountered in chipper-canter lines. From 10° to 90° , the cut was along the grain, and from 90° to 110° , the cut was against the grain. The total cutting length was 105 mm (corresponding to the specimen's length), but the studied length for the subsequent analysis was reduced to an almost central 55 mm length. The 30 last millimeters of the specimen can tend to be torn when the forces are high due to the lack of boundary conditions, and the 20 first millimeters of entry in the specimen are required to reach a steady-state in the cutting forces and chip fragmentation mechanisms. Thus, the entry and the exit of the specimen were not considered in the study in order to focus on the steadiest zone far from the boundaries (Fig. 2).

Because the wood fibers are not straight, even in clear wood, their orientation can vary. The theoretical orientation obtained when machining specimens must be corrected. To minimize the time the specimens are manipulated and to preserve their moisture content (green state), methods such as laser propagation (Nyström 2003; Simonaho *et al.* 2004; Daval *et al.* 2015) were avoided. The measurement of the real grain direction was done “online” on the images recorded during the cut under and above 5 mm of the tool edge, as it was the most solicited area. The method developed to do so is presented in the next subsection. The measurement of the chip thickness was also realized on the images containing the recorded 55 mm-long studied area. The specimen covered 0.1 mm between each image, so the measurement error due to this span was also equal to 0.1 mm.

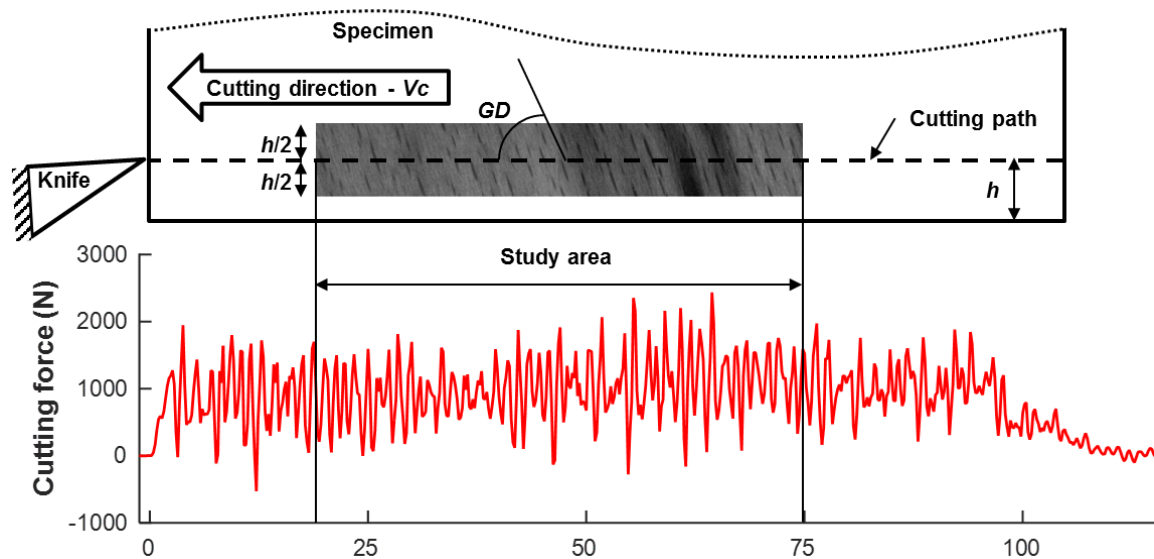


Fig. 2. Study area and example of used data to compute grain direction and cutting forces for one trial

Grain Direction Measurement

The grain direction assessment was inspired by the method developed by Ehrhart *et al.* (2017) in which the innate texture of the beech is used to estimate GD . In this study, pictures were treated using Matlab R2012a (MathWorks, Natick, MA, USA) to detect medullar rays. Images (6 at once, to observe the whole study area) were firstly automatically thresholded into several levels (Fig. 3a and 3b); they were then binarized, conserving only the (darkest) level corresponding to the well-marked medullar rays (Fig. 3c). Medullar rays' contours were drawn and fulfilled to create identified clusters (Fig. 3d). The two main directions of the clusters were determined using a principal components analysis. The eigenvectors of the covariance matrix and their corresponding eigenvalues were calculated. The first eigenvector of each cluster indicates the direction it is elongated the most while the second is its orthogonal vector. Based on the hypothesis that the medullar rays are aligned with the fibers, each eigenvector becomes an indicator of the grain direction. In addition, small contours with internal surfaces lower than 0.03 mm^2 and those with a ratio between the two eigenvalues that is too low (< 15) were removed. These two conditions prevented very small medullar rays, knots, or areas where humidity and color gradients were strong to be considered as medullar rays. This strategy increased the robustness of the image processing and focused on long medullar rays with an angle well defined. The average direction of the remaining clusters were processed and finally averaged to compute the mean grain direction (\overline{GD}) in the specimen.

The absolute necessity of this grain direction correction to increase the accuracy of the study was highlighted and supported by the important differences between GD_{th} and \overline{GD} (Fig. 4a). The errors and relative errors (Fig. 4b) were well centered, with mean error = 0.1° and mean relative error = 1.8% , which was mainly due to the presence of one single outlier with $GD_{th} = 10^\circ$ and $\overline{GD} = 17^\circ$, which produced an important 60% relative error. For 23 specimens, the relative error overcame $\pm 5\%$.

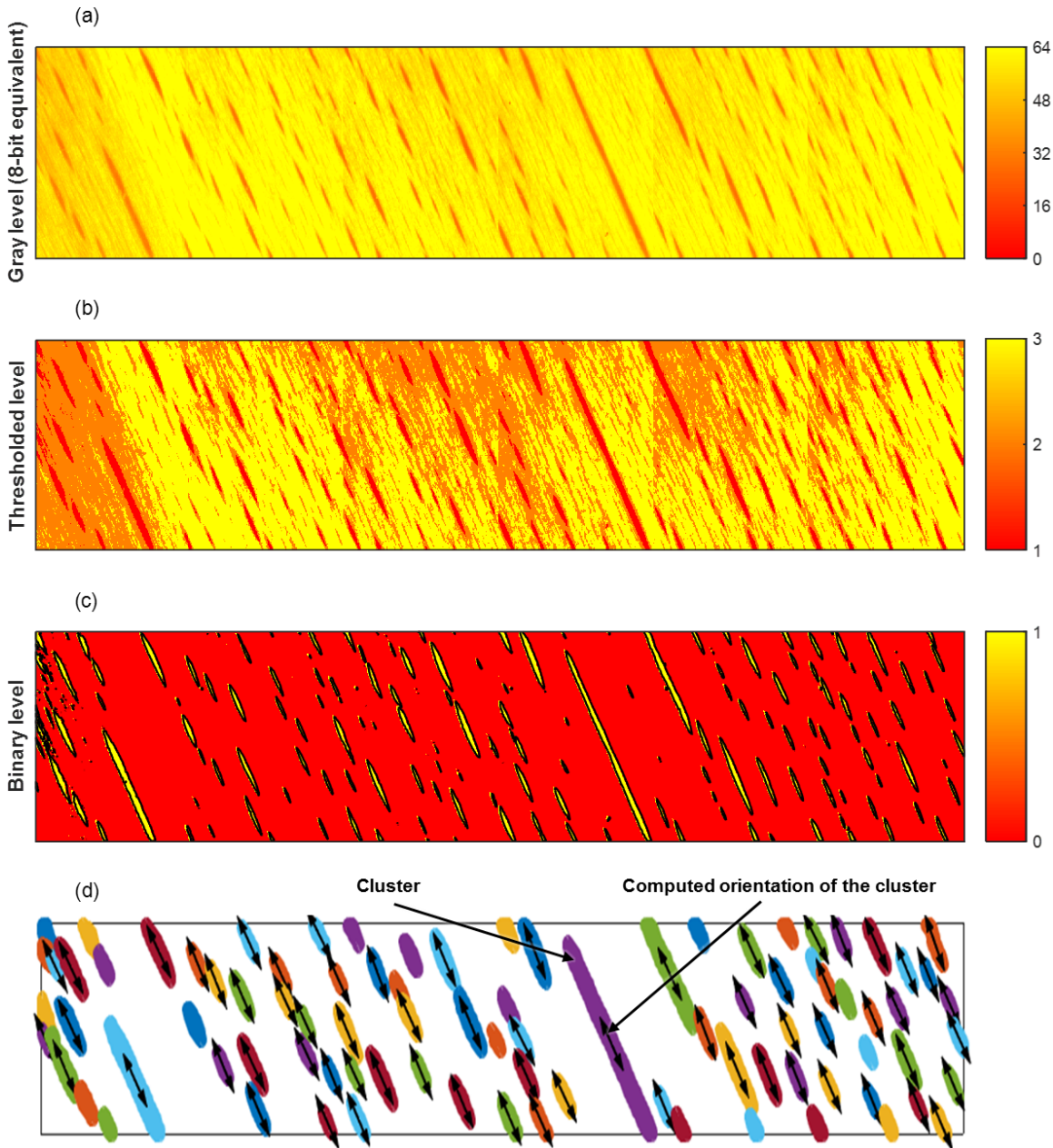


Fig. 3. Image processing state during the grain direction computation: (a) initial image (grayscale converted to 8-bit), (b) 3-level thresholded image, (c) binarized image on which medullar rays contours were detected and drawn (black contour), and (d) clusters and their main directions indicated by the corresponding double-arrow. Clusters where no arrow is associated were not considered in the computation (area too small or shape not elongated enough).

Even with a correct specimen-machining process, the grain direction fluctuation of the wood in the log is sufficient enough to cause fairly high errors if not corrected. This approach and accuracy in the *GD* determination had never been applied to the machining test according to the authors' knowledge.

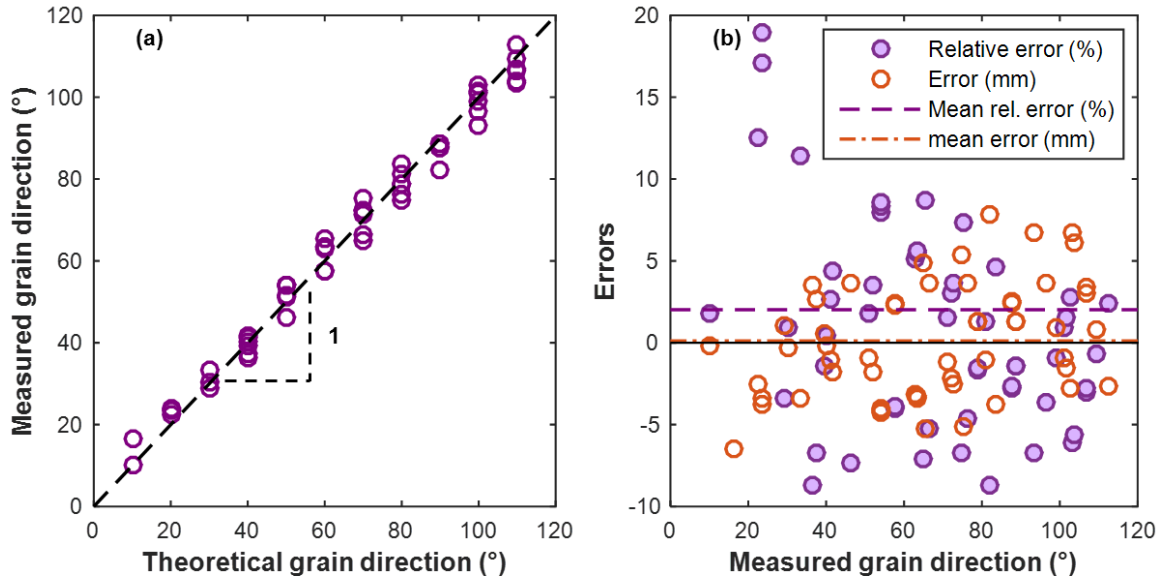


Fig. 4. (a) Measured grain direction versus theoretical grain direction. (b) Errors and relative errors between measured grain direction and theoretical grain direction. One outlier is not plotted (relative error = 60% versus measured grain direction = 17°).

Force Measurement

The dynamometer on which the knife was clamped presented a high resonance, and the cut solicitation spectrum included its natural frequency (1,657 Hz according to conducted hammer tests), leading to very dynamic force signals. To eliminate the dynamic component of the signal, it was averaged over the study area (the dynamic component being a symmetric oscillation around the average signal). Hence, the averaged parallel force (in the cutting direction) and the averaged tearing force (pulling the knife in its clamping direction, orthogonal to the parallel force in the cutting plan) were computed. The resulting force was calculated as the hypotenuse of the two previously quoted averaged forces. Since both the parallel and the tearing forces evolutions towards *GD* exhibit the exact same trends, the resultant force is used as appropriate descriptor for the subsequent analysis. The transversal force, out of the observation plane, was supposed to be null due to the system geometry (every element of the machining setup had been carefully aligned with the machine axis due to the use of a dial test indicator). In practice, over the 46 experiments, the mean transversal force was equal to 5.5 N, and the transversal force was slightly more than 100 times lower than the resulting force (displayed in next section). As a consequence, it was indeed neglected. In the following sections, every force mentioned is the average resulting force. Because of the heterogeneity of the wood samples, the forces were corrected by the specific gravity of the considered specimen with Eq. 3,

$$F_{rc} = \frac{\overline{F_r}}{SG} \times \overline{SG} \quad (3)$$

where F_{rc} is the corrected (by *SG*) average resulting force, $\overline{F_r}$ is the mean resulting force, and \overline{SG} is the mean specific gravity of the whole tested batch.

RESULTS AND DISCUSSION

Impact of the Grain Direction on the Cutting Forces

The mean forces corrected according to the specific gravity of the sample *versus* the measured fiber angle are displayed in Fig. 5 alongside the rough resulting forces. The correction of the cutting forces toward the specific gravity of the specimens was beneficial, as it behaved as expected, allowing the dispersion of the results to be reduced. A linear interpolation of the uncorrected measurements produced a coefficient of determination equal to 0.7, while another linear interpolation of the corrected dataset led to a higher coefficient of determination of 0.75.

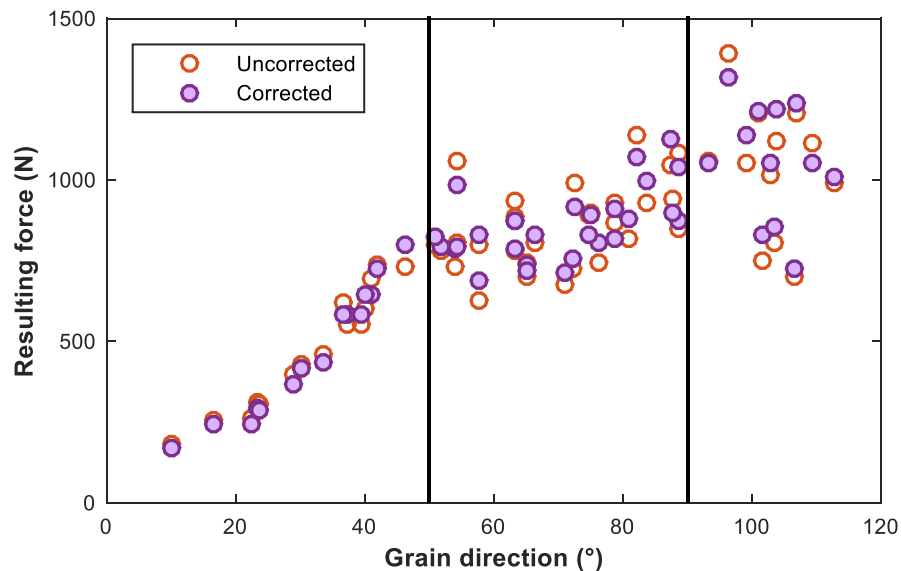


Fig. 5. Mean cutting forces (with and without correction toward specimens' specific gravity) versus the measured grain direction (black bars at 50° and 90° are only visual delimiters)

Along the grain, the corrected mean forces increased as the grain direction increased. Nevertheless, the evolution did not follow the same slope from 10° to 50° as it did from 50° to 90°. The forces increased faster from 10° to 50°, whereas they became nearly constant from 50° to 90°. Once 90° was reached and machining started to be against the grain, the variability of the corrected mean force became higher and no trend could be detected.

Overall, the variability in mean forces was high in the analyzed data. The impact of *MC* on the corrected cutting forces was investigated to determine if it contributed to this variability. However, no major trend was identified, as the literature suggested. Overall, cutting forces in the unfavorable orientation were up to five times higher than in the most favorable cutting conditions.

The 50° and 90° limits were arbitrary but confirmed by analysis of the recorded images. Three main zones appeared with different cutting chip formation mechanisms. However, the transition was smoother than in the mean forces. From 10° to 50°, chip fragmentation occurred with a crack opening starting from the tool edge to the specimen open surface (Fig. 6a), especially for the lowest angles. In the second area, from 50° to 90°, the chip fragmentation was instantaneous and sharp (shorter than the sample time: 1/20,000 s). The main phenomenon seemed to be shearing of the fiber in the longitudinal-

tangential plane (Fig. 6b). From 90° to 110°, the direction of the loading of the chip did not allow it to fragment easily. Instead, the fibers were torn transversally above the tool and longitudinally downstream of the cut higher than the tool edge (Fig. 6c). This last phenomenon explains the variability in the force measured. The large and irregular tearing of the specimen leads to wrenching of the wood. This phenomenon leads to high cutting forces. Conversely, once the wood is wrenched, the tool does not encounter any material over several millimeters, and the cutting forces are null. Therefore, even the mean cutting forces over the 55-mm study area varied a lot from one sample to another because the size of the wrenched material varied. These observations were similar to previous reports (McKenzie 1960; Pfeiffer *et al.* 2014).

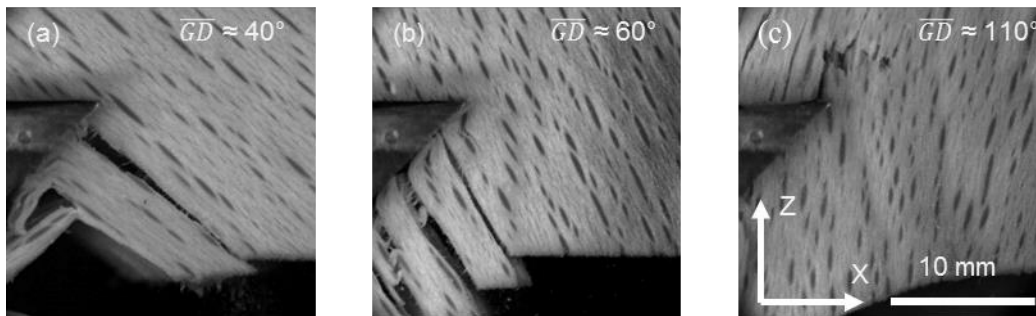


Fig. 6. Evidence of the chip fragmentation mode dependency with the grain direction

Impact of the Grain Direction on the Chip Thickness

From the chip thickness measurements (Fig. 7, one marker corresponds to one chip), mean chip thickness and standard deviation were computed for each cutting experiment according to the grain direction of the sample. Note that for grain directions close to 10° or 110°, the amount of chips generated per experiment was very low (down to a single one).

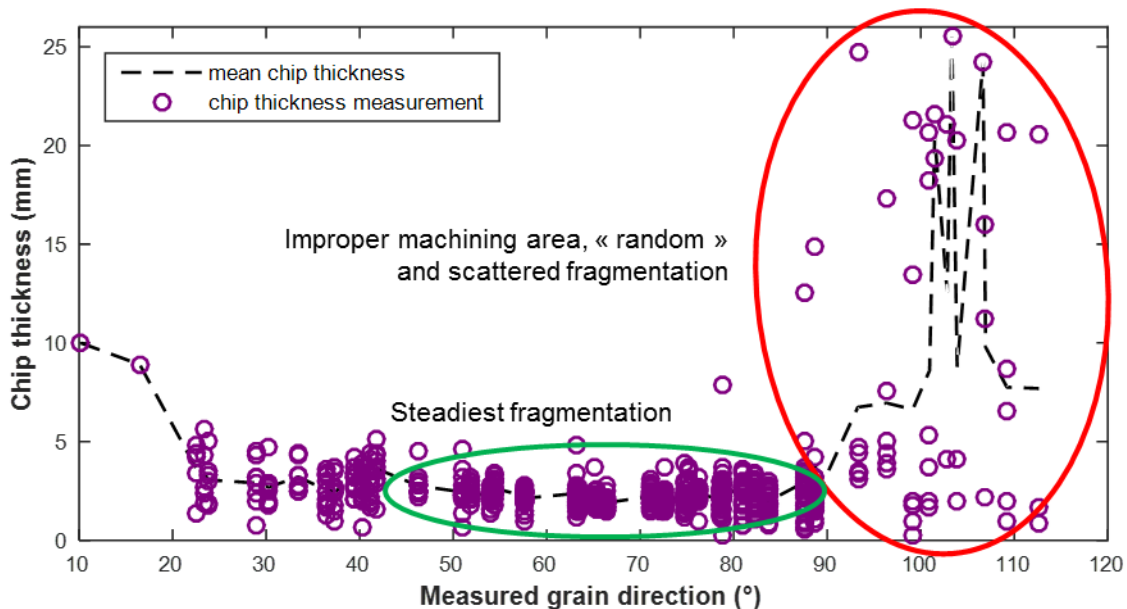


Fig. 7. Chip generated thickness versus the specimen grain direction for $V_c = 2 \text{ m s}^{-1}$, $h = 10 \text{ mm}$, and $b = 10 \text{ mm}$. The tool's rake angle is 45°, and its clearance angle is 5°.

The mean chip thickness decreased quickly from 10° to 20° grain direction and then slowed from 20° to 50°. From 50° to nearly 90°, the chip thickness was stable (30% variation between the minimal and maximal mean thickness in this range). From 90°, the chip thickness increased quickly and became very unstable. This was partly due to the fact that very often small chips succeed a larger one, which generates multiple cracks prior to split. In order to investigate the steadiness of the fragmentation, the focus was drawn to the standard deviation of the chip thickness according to \overline{GD} . \overline{GD} lower than 20° and larger than 85° were removed from this part of the study, as the mechanisms were very different from the rest of the study range, and it appeared obvious to avoid these orientations when machining. Moreover, experiments at those angles did not generate many chips, and standard deviation would be meaningless. Standard deviations were computed on the mentioned range, and a quadratic interpolation was performed (Fig. 8).

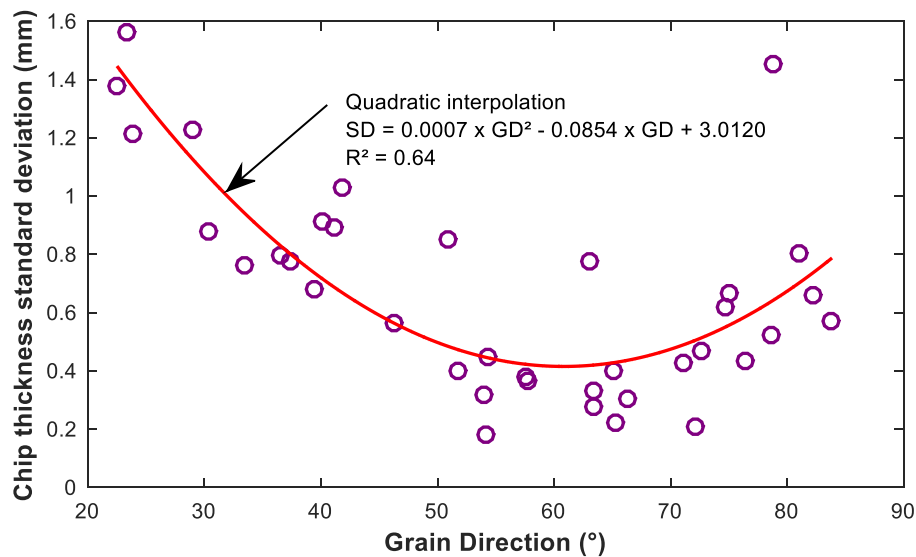


Fig. 8. Chip thickness standard deviation *versus* the specimen grain direction

The quadratic interpolation seemed accurate with a coefficient of determination R^2 of 0.64 (for comparison, a linear interpolation leads to $R^2 = 0.28$). From 25° to 85°, the standard deviation for each trial was similar to that of the mean chip thickness. For instance, it decreased until it reached a minimum between 50° and 70° and increased again beyond this range. The quadratic interpolation pointed to a minimum chip thickness standard deviation of 0.41 mm for $\overline{GD} = 61^\circ$. The coefficient of variation (CV) was computed as the ratio between the mean chip thickness during an experiment and the associated standard deviation. It was not represented as, once again, its behavior was very close to the standard deviation behavior. By fitting another quadratic law, a minimum CV of 0.18 was obtained for $\overline{GD} = 57^\circ$.

CONCLUSIONS

1. To minimize the cutting forces, cutting along the grain is necessary. Cutting against the grain leads to varying forces whose mean value is difficult to predict. A lower angle

between the wood fiber and the cutting direction leads to a lower cutting force. The resulting force was 5 times higher when $\overline{GD} = 90^\circ$ than when $\overline{GD} = 20^\circ$.

2. Fragmentation mechanisms differed highly from low \overline{GD} to high \overline{GD} , but the transition between one phenomenon to another was progressive. Overall, three fragmentations mechanisms impacted the chip geometry; these mechanisms were different for very low \overline{GD} under 50° , \overline{GD} between 50° and 90° , and \overline{GD} above 90° . The chip thickness depended strongly on the mechanism activated.
3. The \overline{GD} range between 50° and 70° was the best-suited range to produce thin chips with a narrow dispersion in their thickness to optimize the targeted final chip valorization in the paper industry. The minimum standard deviation in the chip thickness was reached for $\overline{GD} = 61^\circ$ when interpolating the results, and the minimum variation coefficient was reached for $\overline{GD} = 57^\circ$. Over 85° , the chip thickness was highly scattered and not interesting for a proper exploitation of that waste as an actual economically viable resource.

ACKNOWLEDGMENTS

These works were conducted thanks to the support of the region *Bourgogne Franche-Comté* and the French MESRI. The authors gratefully acknowledge Mr. Pierre-Jean DUREL from MFLS *La Forezienne* for providing cutting tools. The present study was also conducted thanks to the Xylomat Platform funded by the ANR-10-EQPX-16 XYLOFOREST.

REFERENCES CITED

- Akhtaruzzaman, A. F. M, and Virkola, N. E. (1979). "Influence of chip dimensions in kraft pulping. I. Mechanism of movement of chemicals into chips," *Paperi ja Puu* 61(9), 578-580.
- Brännvall, E. (2017). "The limits of delignification in kraft cooking," *BioResources* 12(1), 2081-2107. DOI: 10.15376/biores.12.1.Brannvall
- COPACEL (2017). *Rapport Statistique 2016 de L'industrie Papetière Française*, Union Française des Industries des Cartons, Papiers et Celluloses, (<http://www.copacel.fr>).
- Curti, R., Marcon, B., Collet, R., Lorong, P., Denaud, L. E., and Pot, G. (2017). "Cutting forces and chip formation analysis during green wood machining," in: *23rd IWMS Proceedings*, Warsaw, Poland, pp. 152-161.
- Daval, V., Pot, G., Belkacemi, M., Meriaudeau, F., and Collet, R. (2015). "Automatic measurement of wood fiber orientation and knot detection using an optical system based on heating conduction," *Optics Express* 23(26), 33529-33539. DOI: 10.1364/OE.23.033529
- Ehrhart, T., Steiger, R., and Frangi, A. (2017). "A non-contact method for the determination of fibre direction of European beech wood (*Fagus sylvatica* L.)," *Eur. J. Wood and Wood Prod.* 1-11. DOI: 10.1007/s00107-017-1279-3

- Eyma, F. (2002). *Caractérisation des Efforts de Coupe de Différentes Essences de Bois à L'aide de Leurs Paramètres Mécaniques*, Ph.D. Dissertation, Université Henri Poincaré Nancy 1, Nancy, France.
- FCBA (2017) *Mémento 2017. Supplément Spécial 5th Forest Engineering Conference*, Institut technologique FCBA (Forêt Cellulose Bois-construction Ameublement), (<http://www.fcba.fr/>).
- Felber, G., and Lackner, R. (2005). "Optimization of the production process of sawmill chips for the pulp and paper Industry," in: *17th IWMS Proceedings*, Rosenheim, Germany, pp. 225-240.
- Ghosh, S. C., Hernández, R. E., and Blais, C. (2015). "Effect of knife wear on surface quality of black spruce cants produced by a chipper-canter," *Wood Fiber Sci* 47(4), 1-10.
- Hernández, R. E., and Boulanger, J. (1997). "Effect of the rotation speed on the size distribution of black spruce pulp chips produced by a chipper-canter," *Forest Prod. J.* 47(4), 43-49.
- Hernández, R. E., and Quirion, B. (1995). "Effect of knife clamp, log diameter, and species on the size distribution of pulp chips produced by a chipper-canter," *Forest Prod. J.* 45(7-8), 83-90.
- Hernández, R. E., Passarini, L., and Koubaa, A. (2014). "Effects of temperature and moisture content on selected wood mechanical properties involved in the chipping process," *Wood Sci. Technol.* 48(6), 1281-1301. DOI: 10.1007/s00226-014-0673-9
- Kuljich, S., Hernández, R. E., and Blais, C. (2017). "Effects of cutterhead diameter and log infeed position on size distribution of pulp chips produced by a chipper-canter," *Eur. J. Wood Wood Prod.* 75(5), 747-760. DOI: 10.1007/s00107-016-1150-y
- Kuljich, S., Hernández, R. E., Llavé, A. M., and Koubaa, A. (2013). "Effects of cutting direction, rake angle, and depth of cut on cutting forces and surface quality during machining of balsam fir," *Wood and Fiber Sci.* 45(2), 195-205.
- Laganière, B. (2004). *Effect of Canter Head Rotation Speed, Log Feed Speed and Vertical Position of Logs on Lumber Surface and Chip Quality*, Forintek Canada Corp., Vancouver, BC.
- McKenzie, W. M. (1960). "Fundamental aspects of the wood cutting process," *Forest Prod. J.* 10(9), 447-456.
- Nati, C., Spinelli, R., and Fabbri, P. (2010). "Wood chips size distribution in relation to blade wear and screen use," *Biomass Bioenerg.* 34(5), 583-587. DOI: 10.1016/j.biombioe.2010.01.005
- Nyström, J. (2003). "Automatic measurement of fiber orientation in softwoods by using the tracheid effect," *Comput. Electron. Agr.* 41(1-3), 91-99. DOI: 10.1016/S0168-1699(03)00045-0
- Pfeiffer, R., Collet, R., Denaud, L. E., and Fromentin, G. (2014). "Analysis of chip formation mechanisms and modelling of slabber process," *Wood Sci. Technol.* 49(1), 41-58. DOI: 10.1007/s00226-014-0680-x
- Simonaho, S.-P., Palviainen, J., Tolonen, Y., and Silvennoinen, R. (2004). "Determination of wood grain direction from laser light scattering pattern," *Opt. Laser Eng.* 41(1), 95-103. DOI: 10.1016/S0143-8166(02)00144-6
- Twaddle, A. (1997). "The influence of species, chip length, and ring orientation on chip thickness," *Tappi Journal* 80(6), 123-131.

Williamson, G. B., and Wiemann, M. C. (2010). "Measuring wood specific gravity...Correctly," *Am. J. Bot.* 97(3), 519-524. DOI: 10.3732/ajb.0900243

Article submitted: March 15, 2018; Peer review completed: May 19, 2018; Revised version received and accepted: May 24, 2018; Published: May 27, 2018.

DOI: 10.15376/biores.13.3.5491-5503